REFERENCES

1. Hall P, Holm LE, Lundell G, et al. Cancer risks in thyroid cancer patients. *Br J Cancer* 1991;64:159–163.
2. IARC Study Group on Cancer Risk Among Nuclear Industry Workers. Direct estimates of cancer mortality due to low doses of ionising radiation: an international study. *Lancet* 1994;344:1039–1043.
3. Benua RS, Cical NR, Sonenberg M. The relation of radioiodine dosimetry to results and complications in the treatment of metastatic thyroid cancer. *Am J Roentgenol* 1962;87:171–182.
4. McEwan AC. Absorbed doses in the marrow during ^{131}I therapy. *Br J Radiol* 1977;50:329–331.
5. Agence Internationale de l'Energie Atomique (AIEA). *Biological dosimetry: chromosomal aberration analysis for dose assessment*, technical report series no. 260. Vienna: AIEA; 1986.
6. Finnon P, Lloyd DG, Edwards AA. Fluorescence in situ hybridization detection of chromosomal aberrations in human lymphocytes: applicability to biological dosimetry. *Int J Radiat Biol* 1995;68:429–435.
7. Salassidis K, Georgiadou-Schumacher V, Braselmann H, Müller P, Peter U, Bauchinger M. Chromosome painting in highly irradiated Chernobyl victims: a follow-up study to evaluate the stability of symmetrical translocations and the influence of clonal aberrations for retrospective dose estimation. *Int J Radiat Biol* 1995;68:257–262.
8. Pinkel D, Straume T, Gray J. Cytogenetic analysis using quantitative, high-sensitivity, fluorescence hybridization. *Proc Natl Acad Sci USA* 1986;83:2934–2938.
9. Bender MA, Awa AA, Brooks AL, et al. Current status of cytogenetic procedures to detect and quantify previous exposures to radiation. *Mutat Res* 1988;196:103–159.
10. Lucas JN, Poggensee M, Straume T. The persistence of chromosome translocations in a radiation worker accidentally exposed to tritium. *Cytogenet Cell Genet* 1992;60: 255–256.
11. Lucas JN, Tenjin T, Straume T, et al. Rapid human chromosome aberration analysis using fluorescence in situ hybridization. *Int J Radiat Biol* 1989;56:35–44.
12. M'Kacher R, Legal JD, Schlumberger M, et al. Biological dosimetry in patients treated with 131-radioiodine for differentiated thyroid carcinoma. *J Nucl Med* 1996;37:1860–1864.
13. M'Kacher R, Legal JD, Schlumberger M, et al. Sequential biological dosimetry after a single treatment with iodine-131 for differentiated thyroid carcinoma. *J Nucl Med* 1997;38:377–400.
14. Tucker JD, Ramsey MJ, Lee DA, Minkler JL. Validation of chromosome painting as a biodosimeter in human peripheral lymphocytes following acute exposure to ionizing radiation in vitro. *Int J Radiat Biol* 1993;64:27–37.
15. Lloyd DC, Edwards AA, Prosser JS. Chromosome aberrations induced in human lymphocytes by in vitro acute X and gamma radiation. *Radiat Protection Dosimetry* 1986;15:83–88.
16. Doloy MT. Dosimétrie basée sur le dénombrement des anomalies chromosomiques contenues dans les lymphocytes sanguins. *Radioprotection* 1994;26(suppl 1);171–184.
17. Schmid E, Zitezelsberger H, Braselmann H, Gray JW, Bauchinger M. Radiation-induced chromosome aberrations analysed by fluorescence in situ hybridization with a triple combination of composite whole chromosome-specific DNA probes. *Int J Radiat Biol* 1992;56:673–678.
18. Keldsen N, Mortensen BT, Hassen HS. Bone marrow depression due to ^{131}I treatment of thyroid cancer. *Ugeskr Laeger* 1988;150:2817–2819.
19. Haynie TP, Beierwaltes WH. Hematologic changes observed following ^{131}I for thyroid carcinoma. *J Nucl Med* 1963;4:85–91.
20. Mendelsohn ML, Mayall BH, Bogart E, Moore DH II, Perry BH. DNA content and DNA-based centromere index of the 24 human chromosomes. *Science* 1973;179: 1126–1129.
21. Bender MA, Preston RJ, Leonard RC, Pyatt EE, Gooch PC, Shelby MS. Chromosomal aberration and sister-chromatid exchange frequencies in peripheral lymphocytes of a large human population sample. *Mutat Res* 1988;204:421–433.
22. Bender MA, Preston RJ, Leonard RC, Pyatt EE, Gooch PC. Chromosomal aberration and sister-chromatid exchange frequencies in peripheral lymphocytes of a large human population sample. II. Extension of age range. *Mutat Res* 1989;212:149–154.
23. Anderson D, Jenkinson PC, Dewdney RS, Francis AJ, Godbert P, Butterworth KR. Chromosomal aberrations, mitogen-induced blastogenesis and proliferative rate index in peripheral lymphocytes from 106 control individuals of the U.K. population. *Mutat Res* 1988;204:407–420.
24. Evans HJ. Chromosomal mutations in human populations. *Cytogenet Cell Genet* 1982;33:48–56.
25. A Nordic database on somatic chromosome damage in humans. *Nordic study group on the health risk of somatic chromosome damage. Mutat Res* 1990;241:325–337.
26. Hedner K, Högstedt B, Kolnig AM, Mark-Vendel B, Strömeck B, Mitelman F. Sister chromatid exchanges and structural chromosome aberrations in relation to age and sex. *Hum Genet* 1982;62:305–309.
27. King CM, Gillespie ES, McKenna PG, Barnett YA. An investigation of mutation as a function of age in humans. *Mutat Res* 1994;316:79–90.
28. Lloyd DC, Purrott RJ, Reeder EJ. The incidence of unstable chromosome aberrations in peripheral blood lymphocytes from unirradiated and occupationally exposed people. *Mutat Res* 1980;72:523–532.
29. Tucker JD, Senft JR. Analysis of naturally occurring and radiation-induced breakpoint location in human chromosomes 1, 2 and 4. *Radiat Res* 1994;140:31–36.
30. Annals of the ICRP. *Radiation dose to patients from radiopharmaceuticals*. ICRP publication no. 53. Pergamon Press; 1987.
31. Okada S. Radiation-induced cell death in radiation biochemistry. In: Altman KI, Gerrber GG, Okada S. eds. *Radiation biochemistry*. New York: Academic; 1970:247–307.
32. Schlumberger M, Challeton C, De Vathaire F, et al. Radioactive iodine treatment and external radiotherapy for lung and bone metastases from thyroid carcinoma. *J Nucl Med* 1996;37:598–605.
33. Edmonds CJ, Smith T. The long term hazards of the treatment of thyroid cancer with radioiodine. *Br J Radiol* 1986;59:45–51.
34. Dottorini ME, Lomuscio G, Mazzucchelli L, Vignati A, Colombo L. Assessment of female fertility and carcinogenesis after iodine-131 therapy for differentiated thyroid carcinoma. *J Nucl Med* 1995;36:21–27.

Evaluation of the In Vivo Biodistribution of Yttrium-Labeled Isomers of CHX-DTPA-Conjugated Monoclonal Antibodies

Hisataka Kobayashi, Chuanchu Wu, Tae M. Yoo, Bao-Fu Sun, Debra Drumm, Ira Pastan, Chang H. Paik, Otto A. Gansow, Jorge A. Carrasquillo and Martin W. Brechbiel

Department of Nuclear Medicine, Warren G. Magnuson Clinical Center; and Chemistry Section, Radiation Oncology Branch and Laboratory of Molecular Biology, Division of Basic Sciences, National Cancer Institute, National Institutes of Health, Bethesda, Maryland

We evaluated the in vivo stability and biodistribution of four isomers (CHX-A', CHA-A'', CHX-B' and CHX-B'') of 2-(*p*-isothiocyanatobenzyl)-cyclohexyl-diethylenetriaminepentaacetic acid (CHX-DTPA), a recently developed backbone-substituted derivative of DTPA. **Methods:** The ligands were conjugated to monoclonal antibody B3, a murine IgG1 kappa, and labeled with ^{88}Y at 55.5–66.6 MBq/mg (1.5–1.8 mCi/mg). Nontumor-bearing nude mice were injected intravenously with 55.5–66.6 kBq (1.5–1.8 μCi) of ^{88}Y-labeled B3 conjugates and with ^{125}I-labeled B3 as an internal control. The mice were then killed at 6, 24, 48, 96 and 168 hr postinjection. **Results:** At 168 hr, the concentration of ^{88}Y in processed bone of either CHX-A' [4.6% injected dose (ID)/g] or CHX-A'' (4.0%ID/g) was less than that of either the CHX-B' (21.9%ID/g) or B'' (12.1%ID/g) ligands. The two ligands CHX-B'' and CHX-B' were not acceptable for yttrium labeling of antibody because of their high and progressive bone accumulation. The accumulation of ^{88}Y in bone of CHX-B' was five times greater than that of CHX-A' at 168 hr. The CHX-A'' cleared from the circulation slightly faster than CHX-A' without releasing the yttrium and showed the lowest uptake by bone of any of the four isomers. The accumulation in the other normal organs was similar for all four isomers of ^{88}Y-CHX-B3 conjugates. **Conclusion:** Although the CHX-B'' and CHX-B' were not acceptable for labeling with yttrium, the CHX-A' and CHX-A'' were suitable, indicating that differences in stereochemistry can greatly influence stability of radionuclide in the chelate.

Key Words: DTPA; chelates; stereoisomers; enantiomers; antibody

J Nucl Med 1998; 39:829–836

Received Mar. 12, 1997; revision accepted Aug. 6, 1997.

For correspondence or reprints contact: Jorge A. Carrasquillo, MD, Building 10, Room 1C-401, 10 Center Dr., MSC1180, Bethesda, MD 20892-1180.

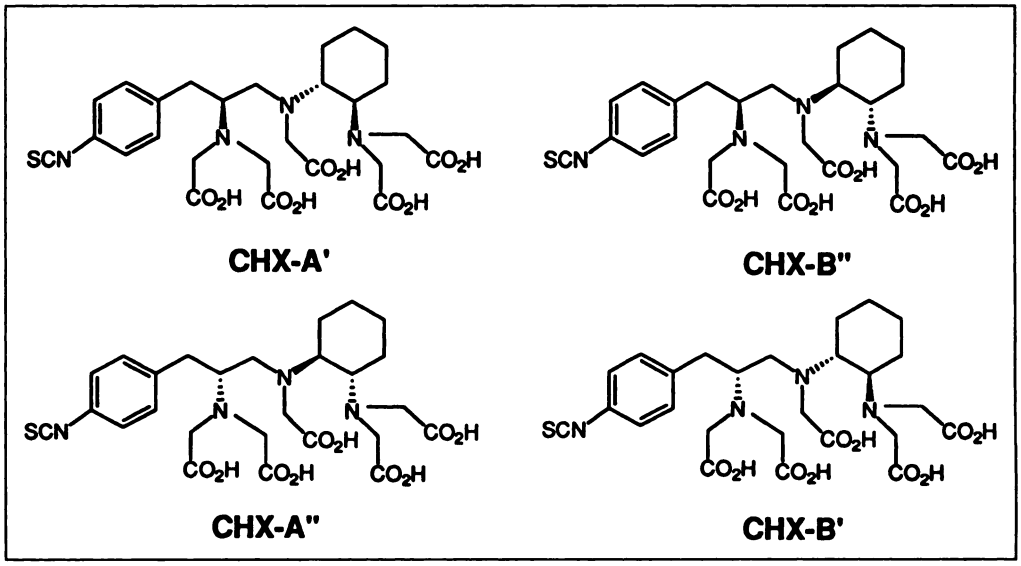

FIGURE 1. Schematic representation of the chemical structure of the bifunctional ligands evaluated in this study. All ligands have an isothiocyanate linker for covalent linkage to the immunoglobulin.

Radiolabeled monoclonal antibodies (MAbs) have undergone extensive evaluation as antitumor agents in both preclinical animal models (*1*) and in clinical trials (*2*). Although ^{131}I has been the most widely used isotope in radioimmunotherapy, limitations of its physical and biological properties have prompted the evaluation of several alternative radionuclides, including beta-emitters such as ^{90}Y (*3–5*), ^{67}Cu (*6*), ^{186}Re (*7*) and ^{177}Lu (*8*) and alpha-emitters such as $^{212/213}$Bi (*9*) and ^{211}At (*10*). Among these, ^{90}Y has been the most extensively studied because of its good chelation properties (*11*), ready availability from a ^{90}Sr/^{90}Y generator (*12*) and physical characteristics (*13*). These characteristics include a 64.1-hr half-life and a pure beta-emission of high energy (E_{max} = 2.28 MeV), which result in higher dose rates and a greater total dose delivered to tumor sites than that delivered by ^{131}I-labeled MAbs (*14*). Furthermore, the considerable path length in tissues of its beta-particles (r_{95} = 5.9 mm) represents a major advantage in solid tumors, in which penetration of antibody molecules is usually poor (*15,16*).

The use of these radiometals requires a chelate that will hold the isotope tightly because, if released from the chelate, these metals would have undesirable targeting and adverse dosimetry (*17–19*). In the case of ^{90}Y, the initial chelates used had been developed for ^{111}In, and their stability for ^{90}Y was suboptimal (*20*). As a result of advances in bifunctional chelate technology for ^{90}Y (*21*), several preclinical studies with those new chelates have indicated that isothiocyanatobenzyl derivatives of DTPA (SCN-Bz-DTPA) have greater stability for ^{90}Y than cyclic anhydride of DTPA, resulting in less bone uptake of ^{90}Y (*20,22–24*). More recently, the 1,4,7,10-tetraazacyclododecane tetraacetic acid (DOTA), a macrocyclic ligand, has been shown to reduce bone accumulation of ^{90}Y further (*25,26*). However, the immunogenicity to DOTA reported in animals (*27*) and humans (*28,29*) and the unfavorable kinetics of its complexation (*30*) have prompted further evaluation of other ligands.

In a previous study, we tested both the in vitro and in vivo stability of the two ^{88}Y-labeled 2-(p-SCN-Bz)-cyclohexyl-DTPA ligands (CHX-A and -B) (*31*). These backbone-substituted derivatives of DTPA (*32*) were compared to other chelates and were found to have favorable stability in chelating yttrium or bismuth. CHX-A bound ^{88}Y more stably in vitro than did 2-(p-SCN-Bz)−6-methyl-DTPA (1B4M-DTPA) and much better than did CHX-B, but it did not bind as well as DOTA (*31*). In vivo studies also showed that CHX-A was more stable than CHX-B. Other studies have shown that both of the CHX DTPAs were good chelates for ^{212}Bi. The CHX-A and -B used previously each consisted of a racemic mixture of two enantiomers. In this study, all four stereoisomers were individually prepared stereospecifically, and their yttrium-complex stability was compared so that we could determine whether there were additional improvements in the biodistribution of ^{88}Y with each individual isomer.

MATERIALS AND METHODS

Monoclonal Antibody

The isolation and characterization of B3 MAb are described in detail elsewhere (*33*). Briefly, B3 is a murine IgG1 kappa that was purified from a serum-free culture medium by ammonium sulfate precipitation and gel-filtration chromatography. B3 reacts with a carbohydrate epitope found on the Le^y and polyfucosylated Le^x antigens. This epitope is present on a large number of glycoproteins and is abundantly and uniformly expressed by most carcinomas (*33*).

Conjugation of Chelates to B3

B3 was concentrated to ~5 mg/ml and dialyzed against 1 liter of 0.05 *M* 4-(2-hydroxyethyl)-1-piperazineethanesulfonic acid and 0.15 *M* NaCl at pH 8.5 for 6 hr. The antibody was then conjugated to the CHX-A′, CHX-A,″ CHX-B′ or CHX-B″ stereoisomers of CHX-DTPA, a recently developed backbone-substituted derivative

TABLE 1
Immunoreactivity Test for Four CHX Conjugates

	CHX-A′-B3	CHX-A″-B3	CHX-B′-B3	CHX-B″-B3
Maximum % specific binding	48.31	51.10	50.85	45.21
Estimated immunoreactivity*	85.64	94.56	93.13	73.25

*Lindmo plot (39).
Data are expressed as a percentage of total radioactivity added per well.

of DTPA (Fig. 1), as described previously (*32,34*). Synthesis of the various stereoisomers are detailed elsewhere (*35*). The average number of chelates per molecule of B3, determined with a spectrophotometric method (*36*), were 2.01, 1.67, 2.47 and 2.34 for CHX-A′, -A″, -B′ and -B″, respectively.

Radiolabeling of B3

Carrier-free ^{88}Y (Los Alamos National Laboratory, Los Alamos, NM) was further purified of metal contaminants by column extraction chromatography (*35*). The four CHX-B3 conjugates were mixed with ^{88}Y at pH 6 for 30 min. The resulting preparations were purified by high-performance liquid chromatography (HPLC) using a TSK 3000 SW size-exclusion column (Toso Hass, Tokyo, Japan) in 0.05 *M* phosphate buffered saline (PBS) at a flow rate of 1.0 ml/min. Labeling yields were 70%–85% for all four conjugates, and their specific activities ranged from 55.5–66.6 MBq/mg (1.5–1.8 mCi/mg).

As an internal control we used B3 labeled with ^{125}I by the chloramine-T method (*37*). Briefly, B3 (100 μg) was mixed in 0.05 *M* phosphate buffer (pH 7.5) with 14.8 MBq (400 μCi) ^{125}I and 12 μg of chloramine-T. After being allowed to react for 5 min, the radiolabeled B3 was purified using a PD-10 column (Pharmacia, Uppsala, Sweden). The specific activity of the ^{125}I-labeled B3 was approximately 111–148 MBq/mg (3–4 mCi/mg). The radiochemical purity of ^{125}I-labeled B3 was >98%, as confirmed by instant thin-layer chromatography and size-exclusion HPLC.

Immunoreactivity

The immunoreactivity of the radiolabeled B3 was determined (*38*). In brief, a constant concentration (3 ng/well) of ^{88}Y-labeled B3 was incubated with various concentrations of A431 cells (50,000–1,000,000 cells/well) in six-well plates. A431 is human epidermoid carcinoma cell line, obtained originally from George Todaro (National Institutes of Health), that expresses high levels of the antigen recognized by B3. The cell-bound activity, corrected for nonspecific binding, was determined, and the immunoreactivity was then calculated by extrapolation to infinite antigen excess conditions (*39*).

Bone-Washing Procedure

The concentration of ^{88}Y in bone was measured by two methods. To determine the concentration of ^{88}Y in cortical bones, we used a modification of the bone-washing method reported by Camera et al. (*31*). Animals (n = 10) were euthanized by CO_2 inhalation and immediately exsanguinated by a cardiac puncture. One femur was then removed from each mouse. The femur was then cut open longitudinally to expose the bone marrow space. To remove the plasma-associated radioactivity, we incubated the fragmented bones in 1.5 ml of PBS for 30 min at room temperature. The bone was allowed to sediment, and the supernatant was aspirated and collected for counting. A second identical wash was then done. The remaining bone was then incubated for 1 hr at 56°C in 1.5 ml of PBS/10% sodium dodecylsulfate (SDS). This sample was then centrifuged at 8000 rpm for 5 min, and the supernatant was collected to extract the "bone marrow"-associated radioactivity. The remaining processed bone was blot-dried and weighed on an analytical balance, and the radioactivity was counted. The counts in the different fractions were expressed as a percentage of the injected dose (ID)/g of processed bone (cortical bone), and the bone-to-blood ratios were determined. In addition, the femur was removed from selected animals and weighed on an analytical balance, and the ^{88}Y was counted before any other processing was performed.

To validate this washing procedure, separate experiments were performed using female athymic mice (6 wk old, n = 6) injected intravenously with one of the following: 185 kBq (5 μCi) of ^{131}I-labeled human serum albumin (HSA) (Merck Frosst Inc., Kirkland, OT, Canada) as a plasma tracer; 185 kBq (5 μCi) of ^{111}In-labeled transferrin as a bone marrow tracer; or 56 kBq (1.5 μCi) of ^{88}Y-citrate as a bone tracer. The ^{111}In-labeled transferrin was obtained by incubating serum from normal mice with $^{111}InCl_3$ at room temperature for 15 min. Groups of six mice were then killed by CO_2 inhalation and exsanguinated at either 2 hr (^{131}I-labeled albumin) or 24 hr postinjection (^{111}In-labeled transferrin; ^{88}Y-citrate). Both femurs were resected and processed as described above. Fractional bone uptake was obtained by separately counting PBS, PBS/10% SDS and bone fractions to determine plasma-associated radioactivity, bone marrow-associated radioactivity and cortical bone uptake, respectively. The counts were also expressed as percentage of total activity in bone.

TABLE 2
Fractional Uptake of Iodine-131-Labeled HSA, Indium-111-Labeled Transferrin and Yttrium-88-Citrate in the Bone and Bone Washes of the Femur

Fraction	^{131}I-HSA	^{111}In-transferrin	^{88}Y-citrate
PBS (%)	68.68 ± 1.48	6.67 ± 0.63	0.46 ± 0.69
SDS (%)	7.29 ± 1.24	22.96 ± 2.11	0.46 ± 0.37
Bone (%)	24.03 ± 1.28	70.37 ± 1.92	99.08 ± 0.98

Fractional bone uptake was determined by separately counting phosphate buffered saline, 10% sodium dodecyl sulfate and bone fraction (see Materials and Methods). Counts were expressed as a percentage of the total activity recovered in the femur. Data are means (%) ± s.d.

Biodistribution Study

All animal studies were performed in 5–6-wk-old female athymic nude mice weighing 16–21 g (Harlan Sprague Dawley, National Cancer Institute, Frederick, MD). All studies were approved by the Clinical Centers' Animal Care and Use Committee. Nontumor-bearing animals were injected with one of the following: ^{88}Y-labeled CHX-A′-B3 [55.5 kBq (1.5 μCi)]; ^{88}Y-labeled CHX-A″-B3 [62.9 kBq (1.7 μCi)]; ^{88}Y-labeled CHX-B′-B3 [62.9 kBq (1.7 μCi)]; or ^{88}Y-labeled CHX-B″-B3 [55.5 kBq (1.5 μCi)]. As an internal control, the animals were coinjected with 148 kBq (4 μCi) of ^{125}I-labeled B3. The combined amount of ^{88}Y- and ^{125}I-labeled B3 was 2 μg.

Groups of five animals receiving each conjugate were then killed at 6, 24, 48, 96 and 168 hr after injection. Aliquots of blood and all major organs were removed and weighed on an analytical balance, and the radioactivity was counted in a well scintillation gamma counter (Autogamma, Packard Instrument Company, Downers Grove, IL). The femur was processed as described above. The whole-body clearance was determined by adding the radioactivity in blood, individual organs and the remaining carcass. Counts were corrected for decay and spillover. Under our counting conditions, ^{125}I and ^{88}Y had 0.004% and 7.2% spillovers into each other's windows.

Additional studies evaluated the blood clearance and distribution in bone of the best two ^{88}Y-labeled CHX conjugates (CHX-A′ and CHX-A″). Ten mice in each group were injected with a total of 2 μg of ^{88}Y-labeled CHX-A′-B3 [62.9 kBq (1.7 μCi)] or CHX-A″-B3 [66.6 kBq (1.8 μCi)] coinjected with ^{125}I-labeled B3 [148 kBq (4 μCi)]. The mice were killed at 96 or 168 hr after injection. Both femurs were weighed separately, and the radioactivity was counted to determine the %ID/g of total nonprocessed bone. The femur was then processed as described above, except that the bone weight used was that of the nonprocessed bone. This procedure was comparable to that of our previous study (*31*). The uptake in the washed bone was expressed as the %ID/g of bone that was in the different fractions (PBS, SDS and bone). This value was obtained

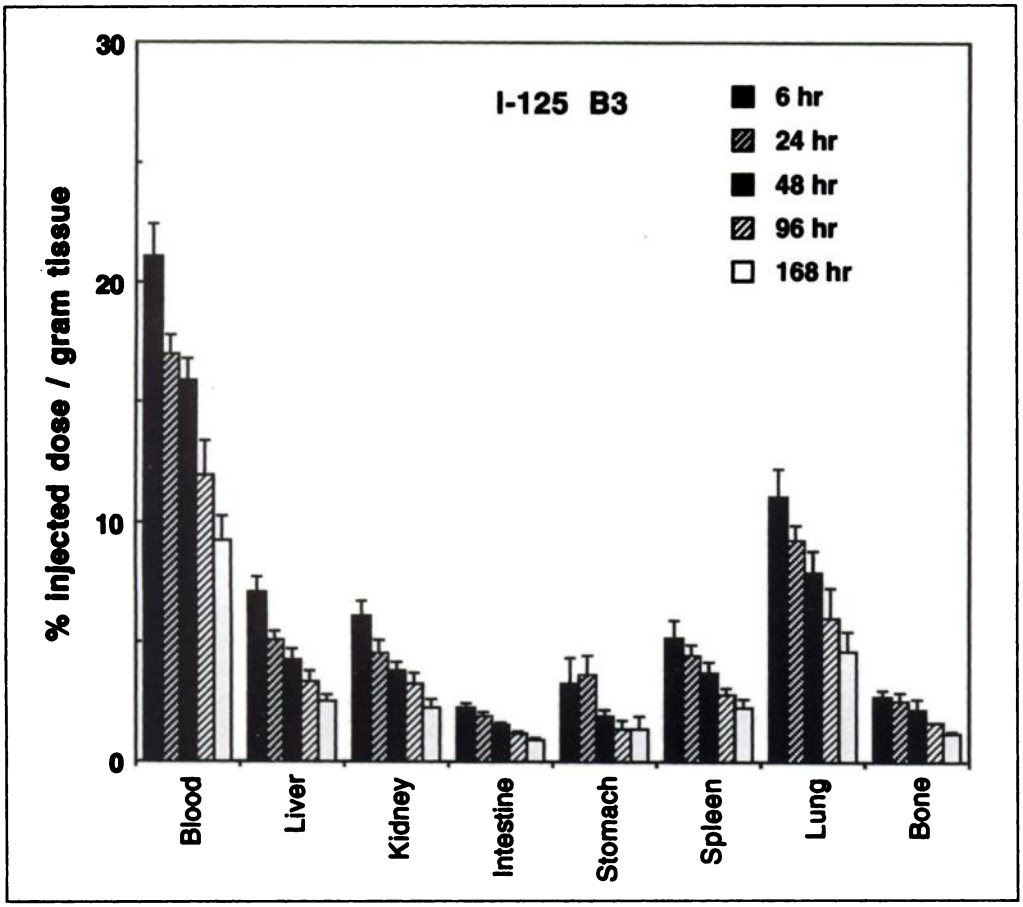

FIGURE 2. Biodistribution of ^{125}I-labeled B3 in non-tumor-bearing mice coinjected with CHX-B''. Animals were killed in groups of five at 6, 24, 48, 96 and 168 hr postinjection. The %ID/g values in all major organs and in blood are shown. Data are means ± s.d. These ^{125}I-labeled B3 data are representative of that seen in the three other groups coinjected with ^{88}Y-labeled CHX conjugates.

by multiplying the %ID/g in the femur by the fractions in the different components. In addition, the activity in the processed bone was divided by the weight of the processed bone (this represented "bone cortex").

Quality Control and In Vivo Stability

Before injection into mice, all radiolabeled B3 preparations were analyzed by HPLC using TSK 2000 size-exclusion columns connected to an on-line gamma detector (γRAM, IN/US Systems, Inc., Fairfield, NJ). The columns were eluted with 0.067 *M* PBS/0.1 *M* KCl buffer (pH 6.8) with a flow rate of 0.5 ml/min. In addition, serum was analyzed at all time points to evaluate the in vivo stability of the radiolabeled B3 conjugates.

Statistical Analysis

We performed the statistical analysis with the one-way analysis of variance, with pairwise comparison using the Bonferroni method (Sigmastat, Jandel Scientific, San Rafael, CA).

RESULTS

Quality Control and In Vivo Stability

Radiochemical purity of all ^{88}Y-labeled B3 preparations was >99%, as determined by size-exclusion HPLC. The analysis of serum samples from all groups of mice showed that the radioactivity recovered was all in the IgG peak, as determined by the size-exclusion HPLC. The immunoreactivity measurements for the four preparations were in the same range (Table 1).

Bone-Washing Procedure

Fractional bone uptakes of ^{131}I-labeled HSA, ^{111}In-labeled transferrin and ^{88}Y-citrate are reported in Table 2. The bone washes in animals receiving ^{131}I-labeled HSA showed that the majority of the radioactivity (68.68%) was released into the PBS wash. The bone washes in animals receiving ^{111}In-transferrin showed that only a mean of 22.96% was in the SDS fraction and 70.37% was retained with the bone. In contrast, the bone washes in animals receiving the ^{88}Y-citrate showed 99.08% accumulation in the bone fraction.

Biodistribution Study

The ^{125}I-labeled B3, which was coinjected as a control, showed similar biodistribution in all four groups of mice receiving the ^{88}Y-labeled antibody conjugates ($p > 0.0001$). Representative ^{125}I-labeled B3 data from one of the four groups coinjected with ^{88}Y-labeled CHX-B''-B3 is shown for comparison (Fig. 2) .

Significant differences were observed in the biodistribution of the four ^{88}Y-labeled CHX-B3 conjugates (Fig. 3). All showed small, but significantly different, blood clearances, as follows: 8.7% ± 0.9%ID/g, 6.6% ± 0.7%ID/g, 6.5% ± 0.3%ID/g and 7.3% ± 0.8%ID/g in blood for CHX-A', CHX-A'', CHX-B' and CHX-B'' at 168 hr, respectively.

At almost all time points, the accumulation of ^{88}Y in all of the other organs except the bone showed a similar distribution pattern. The uptake of all the ^{88}Y-labeled CHX-B3 conjugates in the nonprocessed femur was significantly higher than that of the ^{125}I-labeled B3, with 5.6% ± 0.5%ID/g, 4.8% ± 0.4%ID/g, 16.4% ± 2.1%ID/g and 9.7% ± 1.2%ID/g in the femur at 168 hr for CHX-A', CHX-A'', CHX-B' and CHX-B'', respectively (Fig. 3), whereas the uptake for ^{125}I-labeled B3 was 1.1% ± 0.1%ID/g, 1.1% ± 0.1%ID/g, 1.1% ± 0.2%ID/g and 1.2% ± 0.3%ID/g, respectively.

The cortical bone uptake was also significantly different. Although the accretion of ^{88}Y in the cortical bone increased with time for all ^{88}Y-labeled CHX-B3 conjugates, ^{125}I-labeled B3 showed decreasing cortical bone uptake, with only 0.3% ±

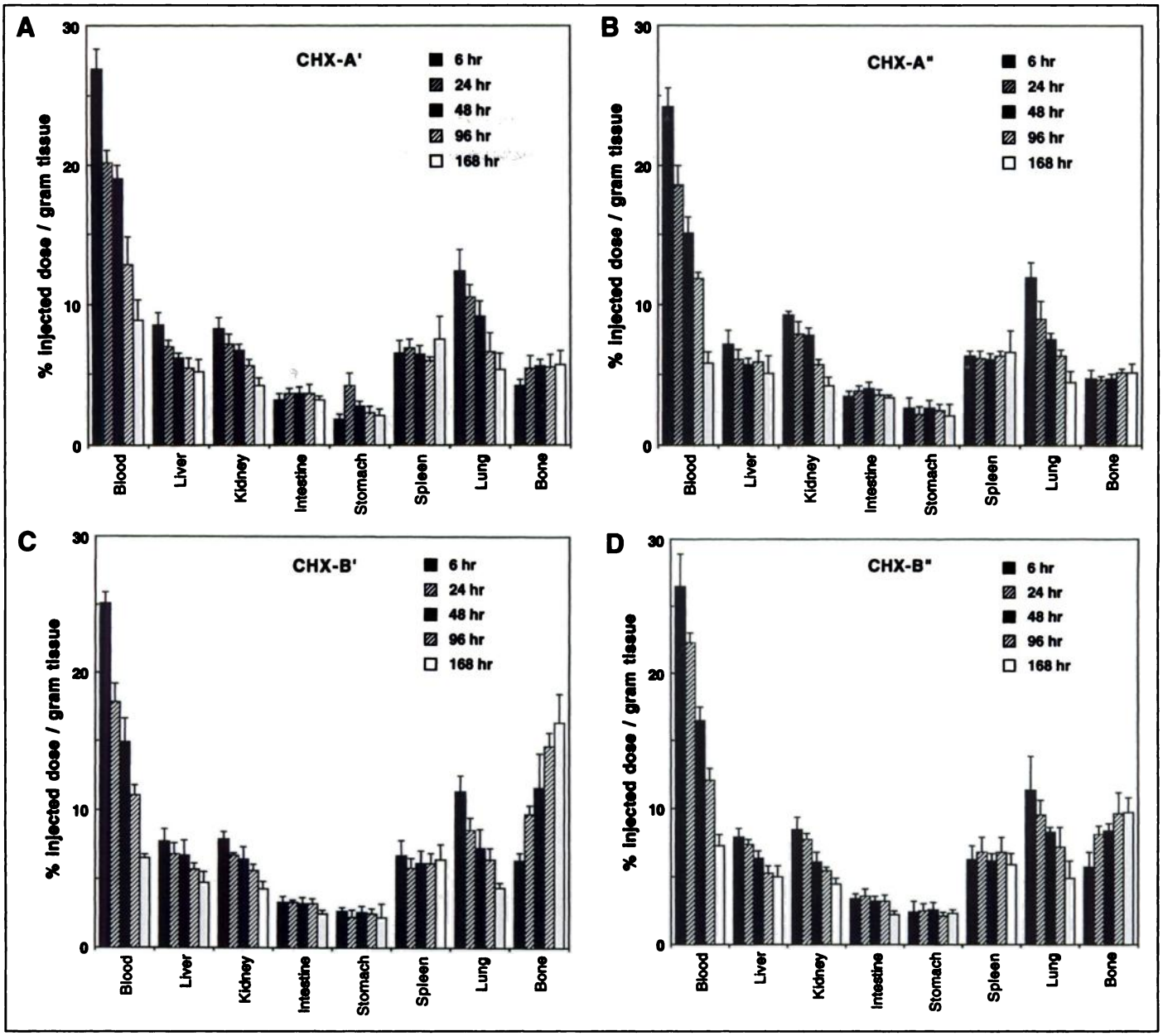

FIGURE 3. Biodistribution of ^{88}Y-labeled CHX-B3-conjugates in non-tumor-bearing mice. Mice were killed in groups of five at 6, 24, 48, 96 and 168 hr postinjection. The %ID/g values in all major organs and in blood are shown for ^{88}Y-labeled CHX-A′-B3 (A), ^{88}Y-labeled CHX-A″-B3 (B), ^{88}Y-labeled CHX-B′-B3 (C) and ^{88}Y-labeled CHX-B″-B3 (D). Data are means ± s.d.

0.1%ID/g at 168 hr. The ^{88}Y uptake in the cortex was significantly different for CHX-A′, CHX-A″, CHX-B′ and CHX-B″, with 5.0% ± 0.6% ID/g, 4.2% ± 0.4%ID/g, 21.9% ± 1.8%ID/g and 12.1% ± 1.5% ID/g, respectively, in the cortex of the processed and dried femur at 168 hr (Fig. 4). The tissue-to-blood ratios showed significant differences in both the nonprocessed femur and processed bone (Table 3).

Although the fractional distribution of ^{88}Y-labeled CHX-A′ and CHX-A″ was similar in the bone (Table 4), the absolute accumulation of ^{88}Y in intact nonprocessed femurs or processed femur was significantly different between CHX-A′ and CHX-A″ at 168 hr after injection of ^{88}Y-labeled CHX-B3 (Table 5). There was little loss of radioactivity during the processing of the femur, as evaluated by a recovery greater than 96% (Table 4).

The whole-body clearance was similar for all four conjugates; a significant difference was found only between CHX-B′ (58% ID) and CHX-A″ (49% ID) remaining in the body at 168 hr (Fig. 5).

DISCUSSION

A major concern with ^{90}Y-labeled MAbs is the selection of a chelate with sufficient thermodynamic and kinetic stability to prevent in vivo loss of the radiometal because dissociated ^{90}Y rapidly accumulates in the bones (*40*) delivering an undesired amount of radiation to the radiosensitive marrow. In our previous study, we reported the stability of complexes formed with racemic mixtures of either CHX-A or CHX-B. The stability of ^{88}Y in CHX-A was slightly greater in vitro than that of the 1B4M chelate. This was confirmed in vivo. The ^{88}Y-labeled CHX-A and 1B4M exhibited very similar bone accumulation. A limited number of studies have been performed evaluating the effect of stereochemistry of a chelate on the stability of isotope retention (*41*). These studies have shown that stereochemistry differences can result in significantly different stability.

In our previous work, the in vitro stability studies predicted the in vivo changes observed between the CHX-A- and CHX-B-labeled MAb. Recent studies comparing the stability of the

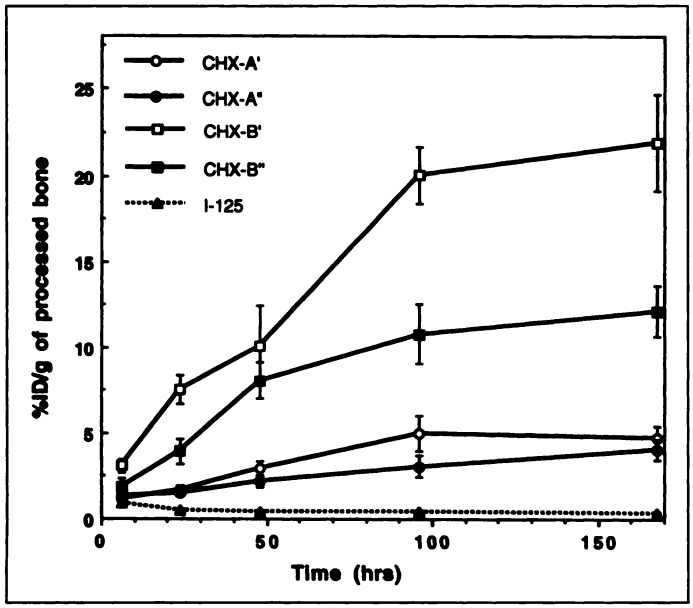

FIGURE 4. Uptake of ^{88}Y in the cortex of the femurs at 6, 24, 48, 96 and 168 hr is shown for all ^{88}Y-labeled CHX-B3 conjugates. Femurs were processed as described in Materials and Methods. Data are expressed as %ID/g of bone cortex (means ± s.d.).

four ^{88}Y-labeled stereoisomers in vitro showed much lower stability of both CHX-B enantiomers when compared to both CHX-A enantiomers. The differences between either CHX-B′ and -B″ or CHX-A′ and -A″ were not significant. This contrasts with the in vivo results, in which marked differences were observed between the two CHX-B enantiomers. The in vivo results for the two CHX-A enantiomers, although different statistically, were very small. These results show that the stability of metal complexes conjugated to proteins in vivo could not be exactly predicted from observations in vitro.

As expected from our previous work, the most striking difference in biodistribution was observed in the bone uptake. Both the %ID/g values in unprocessed bone and in the dried processed bone were significantly different for each of the isomers (Figs. 3 and 4). The concentration of either CHX-A′ or -A″ conjugates in bone was more favorable than either that of CHX-B′ or -B″ conjugates. The differences between the complexes formed with the two CHX-A enantiomers were small but statistically significant. These small differences are real and not due to some technical differences because the concentration of the ^{125}I-labeled B3 control was similar in the femurs of all four groups of mice. In contrast, the differences between the complexes formed with the two CHX-B enantiomers were much larger and increased over time, whereas the differences between the CHX-A′ and -A″ conjugates showed very little increase over time. The trends in uptake between the various conjugates were similar to those of our previous work (Fig. 4), although the absolute concentration in the bone in this study were slightly higher than in the previous study (*31*). These differences are likely to be technical in nature and may be related to small differences in handling the bone because small changes in the bone weight could account for them.

Possible explanations to account for the in vivo stability differences observed between the four stereoisomeric CHX-DTPA ^{88}Y-labeled conjugates are clearly rooted in the configuration of the ligands themselves. The large differences between the racemates CHX-A and -B are simply attributable to their diastereomeric nature, wherein CHX-B, by virtue of configuration, forms less stable yttrium complexes than the

TABLE 3
Normal Tissue-to-Blood Ratio of Yttrium-88-Labeled CHX-B3 and Iodine-125-Labeled B3

Organ	Time (hr)	Compounds					
		CHX-A′	CHX-A″	CHX-B′	CHX-B″	^{125}I	p*
Liver	6	0.32 ± 0.03	0.30 ± 0.05	0.31 ± 0.04	0.29 ± 0.03	0.33 ± 0.02	ns
	24	0.35 ± 0.02	0.33 ± 0.02	0.38 ± 0.06	0.33 ± 0.02	0.39 ± 0.02	ns
	48	0.32 ± 0.03	0.38 ± 0.04	0.45 ± 0.07	0.39 ± 0.01	0.27 ± 0.03	ns
	96	0.43 ± 0.08	0.50 ± 0.06	0.51 ± 0.07	0.43 ± 0.02	0.29 ± 0.07	ns
	168	0.59 ± 0.14	0.90 ± 0.31	0.72 ± 0.13	0.68 ± 0.12	0.27 ± 0.03	ns
Kidney	6	0.31 ± 0.04	0.38 ± 0.01	0.32 ± 0.03	0.32 ± 0.04	0.29 ± 0.04	ns
	24	0.35 ± 0.03	0.42 ± 0.03	0.38 ± 0.03	0.35 ± 0.02	0.26 ± 0.03	ns
	48	0.35 ± 0.03	0.52 ± 0.04	0.43 ± 0.02	0.37 ± 0.03	0.24 ± 0.03	ns
	96	0.44 ± 0.08	0.48 ± 0.04	0.51 ± 0.02	0.45 ± 0.02	0.27 ± 0.07	ns
	168	0.48 ± 0.04	0.72 ± 0.12	0.66 ± 0.08	0.62 ± 0.08	0.24 ± 0.02	ns
Intestine	6	0.12 ± 0.01	0.14 ± 0.02	0.13 ± 0.01	0.13 ± 0.01	0.11 ± 0.01	ns
	24	0.18 ± 0.01	0.21 ± 0.03	0.19 ± 0.01	0.16 ± 0.02	0.11 ± 0.01	ns
	48	0.19 ± 0.02	0.27 ± 0.04	0.22 ± 0.04	0.19 ± 0.02	0.10 ± 0.01	ns
	96	0.29 ± 0.08	0.30 ± 0.04	0.29 ± 0.05	0.27 ± 0.05	0.10 ± 0.02	ns
	168	0.37 ± 0.07	0.58 ± 0.09	0.38 ± 0.04	0.31 ± 0.07	0.10 ± 0.00	<0.0001
Bone (nonprocessed)	6	0.16 ± 0.01	0.20 ± 0.03	0.25 ± 0.03	0.21 ± 0.03	0.13 ± 0.01	<0.0001
	24	0.27 ± 0.05	0.25 ± 0.01	0.55 ± 0.07	0.36 ± 0.02	0.14 ± 0.02	<0.0001
	48	0.30 ± 0.03	0.31 ± 0.04	0.78 ± 0.16	0.51 ± 0.06	0.14 ± 0.03	ns
	96	0.44 ± 0.08	0.43 ± 0.03	1.33 ± 0.05	0.80 ± 0.14	0.14 ± 0.02	ns
	168	0.64 ± 0.06	0.82 ± 0.11	2.54 ± 0.40	1.34 ± 0.21	0.12 ± 0.01	<0.0001
Bone cortex (processed)	6	0.04 ± 0.01	0.05 ± 0.00	0.13 ± 0.02	0.07 ± 0.01	0.04 ± 0.01	<0.0001
	24	0.09 ± 0.01	0.08 ± 0.02	0.40 ± 0.02	0.19 ± 0.04	0.03 ± 0.01	<0.0001
	48	0.16 ± 0.03	0.15 ± 0.02	0.73 ± 0.21	0.47 ± 0.03	0.03 ± 0.01	ns
	96	0.41 ± 0.10	0.27 ± 0.06	1.77 ± 0.06	0.94 ± 0.18	0.04 ± 0.01	<0.0001
	168	0.57 ± 0.08	0.64 ± 0.05	3.30 ± 0.47	1.73 ± 0.26	0.04 ± 0.01	<0.0001

*Differences are calculated between CHX conjugates only (not ^{125}I-labeled B3).
Data are mean ± s.d.; n = 5 in each group at each time point; ns = not significant.

TABLE 4
Fractional Uptake of Yttrium-88-Labeled CHX-A′-B3 Compared to Yttrium-88-Labeled CHX-A″-B3 in Bone

	96 hr				168 hr			
	PBS	SDS	Bone	Recovery*	PBS	SDS	Bone	Recovery
CHX-A′	20.2 ± 1.8	5.6 ± 1.5	70.8 ± 3.3	96.6 ± 2.1	11.7 ± 1.2	4.0 ± 1.2	82.5 ± 3.7	98.3 ± 2.3
CHX-A″	20.8 ± 4.1	4.4 ± 0.8	72.6 ± 4.5	97.9 ± 2.1	10.7 ± 1.2	3.8 ± 1.2	84.4 ± 3.2	98.8 ± 2.2

*Recovery is the percentage of the original activity that is accumulated by summing the activity in the three fractions.
Data are means (%) ± s.d.; n = 10 in each group at each time point ($p > 0.04$); PBS = phosphate buffered saline; SDS = sodium dodecyl sulfate.

TABLE 5
Percentage of Injected Dose Per Gram of Yttrium-88-Labeled CHX-A′-B3 Compared to Yttrium-88-Labeled CHX-A″-B3 in Normal Nude Mice 96 and 168 Hr After Injection (n = 10)

	96 hr				168 hr			
	Blood	Bone*	Bone cortex†	Washed bone‡	Blood	Bone	Bone cortex	Washed bone
CHX-A′	13.6 ± 1.0	4.9 ± 0.3	3.3 ± 0.4	3.5 ± 0.3	8.7 ± 0.9	5.6 ± 0.5	5.0 ± 0.6	4.6 ± 0.4
CHX-A″	11.5 ± 0.8§	4.6 ± 0.4	2.7 ± 0.4§	3.3 ± 0.4	6.6 ± 0.7§	4.8 ± 0.4§	4.2 ± 0.4§	4.0 ± 0.4§

*The activity in the nonprocessed femur.
†The activity in the processed femur using the weight of dried processed bone.
‡The activity in the nonprocessed femur multiplied by the fraction in the bone compartment.
§$p < 0.01$ compared with CHX-A′.
Data are means ± s.d.; n = 10 in each group at each time point.

CHX-A. As expected, preliminary modeling of the enantiomers has yet to yield any distinct, obvious links to differences in stability between the two complexes. An explanation for the differences that were observed between the ^{88}Y-labeled conjugates formed using enantiomeric ligands is not available at this time.

Although we attempted to improve our bone processing procedure over that described by Camera et al. (*31*), some limitations were still obvious. As shown previously, our method could not remove all the ^{131}I-HSA that was expected to be in the marrow space based on plasma accumulation, nor could we remove the bone marrow-associated ^{111}In, although the current method represented an improvement over the previous one in removing ^{111}In from the marrow. Nevertheless, despite the limitations, our procedure did not underestimate the bone-associated ^{88}Y because the validation study showed that >99% of the ^{88}Y-citrate was recovered in the bone fraction. In mice injected with ^{88}Y-labeled CHX-A″-B3, dried cortical bone uptake at 168 hr was two and three times less than that observed for ^{88}Y-labeled CHX-B′-B3 and ^{88}Y-labeled CHX-B″-B3, respectively (Fig. 3). This is probably the result of subtle unfavorable steric hindrance present in one configuration but not in the other. While these findings mirrored those of the in vitro serum stability study, differences in the in vivo stability of the ^{88}Y-labeled B3-conjugates were not detected by our HPLC analysis of serum samples, which failed to detect species other than intact IgG. This does not represent an unusual finding, and it is probably due to the fact that free yttrium is rapidly removed from the blood and taken up by the bone.

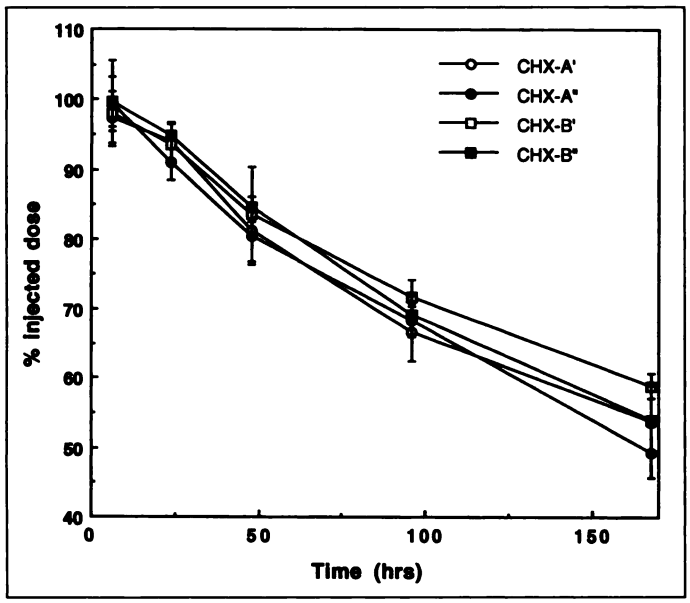

FIGURE 5. The whole-body retention of all four conjugates. Data are expressed as %ID (means ± s.d.).

CONCLUSION

Our study confirms that ^{88}Y-labeled CHX-A conjugates are more stable than the CHX-B conjugates. Therefore, for clinical use with ^{90}Y, neither of the CHX-B conjugates is acceptable. Given that the stereochemistry of preparing any of these conjugates independently is not a major limitation, we recommend the CHX-A″, which showed the least bone uptake and can be used for other radiometals, such as the alpha-emitters ^{212}Bi and ^{213}Bi. These studies emphasize the importance of stereochemistry in evaluating and selecting chelates for clinical applications.

REFERENCES

1. Buchsbaum DJ, Langmuir VK, Wessels BW. Experimental radioimmunotherapy. *Med Phys* 1993;20:551–567.
2. Larson SM, Divgi CR, Scott AM. Overview of clinical radioimmunodetection of human tumors. *Cancer* 1994;73:832–835.
3. Sharkey RM, Kaltovich FA, Shih LB, Fand I, Govelitz G, Goldenberg DM. Radioimmunotherapy of human colonic cancer xenografts with ^{90}Y-labeled monoclonal antibodies to carcinoembryonic antigen. *Cancer Res* 1988;48:3270–3275.
4. Lee YC, Washburn LC, Sun TT, et al. Radioimmunotherapy of human colorectal carcinoma xenografts using ^{90}Y-labeled monoclonal antibody CO17–1A prepared by two bifunctional chelate techniques. *Cancer Res* 1990;50:4546–4551.
5. Schmidberger H, Buchsbaum DJ, Blazar BR, Everson P, Vallera DA. Radiotherapy in

mice with yttrium-90-labeled anti-Ly1 monoclonal antibody: therapy of the T cell lymphoma EL4. *Cancer Res* 1991;51:1883–1890.
6. Deshpande SV, DeNardo SJ, Meares CF, et al. Copper-67-labeled monoclonal antibody Lym-1, a potential radiopharmaceutical for cancer therapy: labeling and biodistribution in RAJI tumored mice. *J Nucl Med* 1988;29:217–225.
7. Beaumier PL, Venkatesan P, Vanderheyden JL, et al. ^{86}Re radioimmunotherapy of small cell lung carcinoma xenografts in nude mice. *Cancer Res* 1991;51:676–681.
8. Schlom J, Siler K, Milenic DE, et al. Monoclonal antibody-based therapy of a human tumor xenograft with a ^{77}lutetium-labeled immunoconjugate. *Cancer Res* 1991;51: 2889–2896.
9. Kozak RW, Atcher RW, Gansow OA, Friedman AM, Hines JJ, Waldmann TA. Bismuth-212-labeled anti-Tac monoclonal antibody: alpha-particle-emitting radionuclides as modalities for radioimmunotherapy. *Proc Natl Acad Sci USA* 1986;83:474–478.
10. Zalutsky MR, Garg PK, Friedman HS, Bigner DD. Labeling monoclonal antibodies and F(ab') fragments with the alpha-particle-emitting nuclide astatine-211: preservation of immunoreactivity and in vivo localizing capacity. *Proc Natl Acad Sci USA* 1989;86:7149–7153.
11. Martell AE, Smith RM. *Critical stability constants. Amino acids*, vol. 1. New York: Plenum Press; 1974:281–284.
12. Chinol M, Hnatowich DJ. Generator-produced yttrium-90 for radioimmunotherapy. *J Nucl Med* 1987;28:1465–1470.
13. Wessels BW, Rogus RD. Radionuclide selection and model absorbed dose calculations for radiolabeled tumor associated antibodies. *Med Phys* 1984;11:638–645.
14. Klein JL, Nguyen TH, Laroque P, et al. Yttrium-90 and iodine-131 radioimmunoglobulin therapy of an experimental human hepatoma. *Cancer Res* 1989;49:6383–6389.
15. Juweid M, Neumann R, Paik C, et al. Micropharmacology of monoclonal antibodies in solid tumors: direct experimental evidence for a binding site barrier. *Cancer Res* 1992;52:5144–5153.
16. Saga T, Neumann RD, Heya T, et al. Targeting cancer micrometastases with monoclonal antibodies: a binding-site barrier. *Proc Natl Acad Sci USA* 1995;92:8999–9003.
17. Stewart JS, Hird V, Snook D, et al. Intraperitoneal yttrium-90-labeled monoclonal antibody in ovarian cancer. *J Clin Oncol* 1990;8:1941–1950.
18. Stewart JS, Hird V, Snook D, et al. Intraperitoneal radioimmunotherapy for ovarian cancer: pharmacokinetics, toxicity, and efficacy of I-131 labeled monoclonal antibodies. *Int J Radiat Oncol Biol Phys* 1989;16:405–413.
19. Hnatowich DJ, Virzi F, Doherty PW. DTPA-coupled antibodies labeled with yttrium-90. *J Nucl Med* 1985;26:503–509.
20. Roselli M, Schlom J, Gansow OA, et al. Comparative biodistributions of yttrium- and indium-labeled monoclonal antibody B72.3 in athymic mice bearing human colon carcinoma xenografts. *J Nucl Med* 1989;30:672–682.
21. Brechbiel MW, Gansow OA, Atcher RW, et al. Synthesis of 1-(p-isothiocyanatobenzyl) derivatives of DTPA and EDTA. Antibody labeling and tumor-imaging studies. *Inorg Chem* 1986;25:2772–2781.
22. Kozak RW, Raubitschek A, Mirzadeh S, et al. Nature of the bifunctional chelating agent used for radioimmunotherapy with yttrium-90 monoclonal antibodies: critical factors in determining in vivo survival and organ toxicity. *Cancer Res* 1989;49:2639–2644.
23. Sharkey RM, Motta-Hennessy C, Gansow OA, et al. Selection of a DTPA chelate conjugate for monoclonal antibody targeting to a human colonic tumor in nude mice. *Int J Cancer* 1990;46:79–85.
24. Washburn LC, Sun TT, Lee YC, et al. Comparison of five bifunctional chelate techniques for ^{90}Y-labeled monoclonal antibody CO17-1A. *Int J Radiat Appl Instrum B* 1991;18:313–321.
25. Deshpande SV, Subramanian R, McCall MJ, DeNardo SJ, DeNardo GL, Meares CF. Metabolism of indium chelates attached to monoclonal antibody: minimal transchelation of indium from benzyl-EDTA chelate in vivo. *J Nucl Med* 1990;31:218–224.
26. Harrison A, Walker CA, Parker D, et al. The in vivo release of ^{90}Y from cyclic and acyclic ligand–antibody conjugates. *Int J Radiat Appl Instrum B* 1991;18:469–476.
27. Watanabe N, Goodwin DA, Meares CF, et al. Immunogenicity in rabbits and mice of an antibody-chelate conjugate: comparison of (S) and (R) macrocyclic enantiomers and an acyclic chelating agent. *Cancer Res* 1994;54:1049–1054.
28. Kosmas C, Snook D, Gooden CS, et al. Development of humoral immune responses against a macrocyclic chelating agent (DOTA) in cancer patients receiving radioimmunoconjugates for imaging and therapy. *Cancer Res* 1992;52:904–911.
29. Kosmas C, Maraveyas A, Gooden CS, Snook D, Epenetos AA. Anti-chelate antibodies after intraperitoneal yttrium-90-labeled monoclonal antibody immunoconjugates for ovarian cancer therapy. *J Nucl Med* 1995;36:746–753.
30. Kodama M, Koike T, Mahatma AB, Kimura E. Thermodynamic and kinetic studies of lanthanide complexes of 1,4,7,10,13-pentaazacyclopentadecane-N, N', N'',N''',N''', hexaacetic acid. *Inorg Chem* 1991;30:1270–1273.
31. Camera L, Kinuya S, Garmestani K, et al. Evaluation of the serum stability and in vivo biodistribution of CHX-DTPA and other ligands for yttrium labeling of monoclonal antibodies. *J Nucl Med* 1994;35:882–889.
32. Brechbiel MW, Gansow OA. Synthesis of C-functionalized trans-cyclohexyldiethylenetriaminepentaacetic acids for labelling of monoclonal antibodies with the bismuth-212 α-particle emitter. *J Chem Soc Perkin Trans* 1992;1:1173–1178.
33. Pastan I, Lovelace ET, Gallo MG, Rutherford AV, Magnani JL, Willingham MC. Characterization of monoclonal antibodies B1 and B3 that react with mucinous adenocarcinomas. *Cancer Res* 1991;51:3781–3787.
34. Mirzadeh S, Brechbiel MW, Atcher RW, Gansow OA. Radiometal labeling of immunoproteins: covalent linkage of 2-(4-isothiocyanatobenzyl) diethylenetriaminepentaacetic acid ligands to immunoglobulin. *Bioconjug Chem* 1990;1:59–65.
35. Wu C, Kobayashi H, Sun B-F, et al. Stereochemical influence on the stability of radio-metal complexes in vivo. Synthesis and evaluation of the four stereoisomers of 2-(*p*-nitrobenzyl)-*trans*-CyDTPA. *Bioorg Med Chem* 1997;5:1925–1934.
36. Pippin CG, Parker TA, McMurry TJ, Brechbiel MW. Spectrophotometric method for the determination of a bifunctional DTPA ligand in DTPA-monoclonal antibody conjugates. *Bioconjug Chem* 1992;3:342–345.
37. Greenwood FC, Hunter WM, Glover JS. The preparation of ^{131}I-labelled human growth hormone of high specific radioactivity. *Biochem J* 1963;89:114–123.
38. Camera L, Kinuya S, Pai LH, et al. Preclinical evaluation of ^{111}In-labeled B3 monoclonal antibody: biodistribution and imaging studies in nude mice bearing human epidermoid carcinoma xenografts. *Cancer Res* 1993;53:2834–2839.
39. Lindmo T, Boven E, Cuttitta F, Fedorko J, Bunn PA Jr. Determination of the immunoreactive fraction of radiolabeled monoclonal antibodies by linear extrapolation to binding at infinite antigen excess. *J Immunol Methods* 1984;72:77–89.
40. Jowsey J, Rowland RE, Marshall JH. The deposition of rare earths in bone. *Radiat Res* 1958;8:490–501.
41. Madsen SL, Bannochie CJ, Martell AE, Mathias CJ, Welch MJ. Investigation of physicochemical and in-vivo behavior of diastereomeric iron-59, gallium-68, and indium-111-EHPG trivalent metal complexes. *J Nucl Med* 1990;31:1662–1668.

Divalent Cobalt as a Label to Study Lymphocyte Distribution Using PET and SPECT

Jakob Korf, Lammy Veenma-van der Duin, Rikje Brinkman-Medema, Anita Niemarkt and Lou F.M.H. de Leij

Department of Biological Psychiatry, Groningen School of Behaviour and Cognitive Neurosciences, Groningen, and Clinical Immunology, Groningen School of Drug Exploration, University Hospital, Groningen, the Netherlands

PET and SPECT allow the study of the distribution of lymphocytes in living humans, provided that these cells are adequately prelabeled ex vivo. Such a labeling technique should not only be nontoxic to lymphocytes but it also should take into consideration that their kinetics are such that radioactivity must be followed for at least 24 hr. We describe the potential of divalent cobalt isotopes ($^{55}Co^{2+}$, half-life 17.5 hr for PET; $^{57}Co^{2+}$, half-life 270 days for SPECT) for labeling lymphocytes. **Methods:** Isolated rat lymphocytes were incubated with $^{57}CoCl_2$ with or without unlabeled $CoCl_2$ or $CaCl_2$ carrier or other compounds. In some experiments, the accumulation of radioactive cobalt and calcium in lymphocytes was determined in the presence of phorbol myristate acetate alone, calcimycine alone or in combination. The toxicity of cobalt to lymphocytes was assessed with the trypan blue exclusion test and by assessing their proliferative capacity using radioactive thymidine incorporation as a readout. Biodistribution of cobalt-labeled lymphocytes was determined with postmortem analysis and compared with that of the free (nonlymphocyte-bound) tracer. **Results:** At high concentrations (more than 100 × necessary for adequate labeling), cobalt was not cytotoxic. Incubation of labeled lymphocytes in tissue culture medium for 24 hr in vitro showed a loss of less than half of the incorporated cobalt radioactivity. Twenty-four hours after in vitro labeling of lymphocytes and intravenous injection, radioactivity accumulated not only in the liver, kidney and bladder of the rat but in the spleen and lungs, which differed from the distribution of the free tracer. Uptake and binding to rat lymphocytes of Co^{2+} partly mimicked that of Ca^{2+}. The binding of cobalt, however, was stronger and nonsaturable. **Conclusion:** These results warrant further exploration of cobalt as a PET or SPECT label of human lymphocytes.

Key Words: lymphocytes; cobalt; PET; SPECT; calcium

J Nucl Med 1998; 39:836–841

Received Apr. 1, 1997; revision accepted Aug. 6, 1997.

For correspondence or reprints contact: Jakob Korf, PhD, Department of Biological Psychiatry and Neuro-PET Coordination, Groningen University Hospital, P.O. Box 30.001, 9700 RB Groningen, the Netherlands.